

The Highest D Value for a Mn^{II} Ion: Investigation of a Manganese(II) Polyoxometalate Complex by High-Field Electron Paramagnetic Resonance

Céline Pichon,[†] Pierre Mialane,^{*,†} Eric Rivière,[‡] Guillaume Blain,[‡] Anne Dolbecq,[†] Jérôme Marrot,[†] Francis Sécheresse,[†] and Carole Duboc^{*,§,||}

Institut Lavoisier, UMR 8180, Université de Versailles Saint-Quentin, 45 Avenue des Etats-Unis, 78035 Versailles Cedex, France, Institut de Chimie Moléculaire et des Matériaux d'Orsay, UMR 8182, Equipe Chimie Inorganique, Université Paris-Sud, 91405 Orsay, France, High Magnetic Field Laboratory, CNRS, UPR 5021, BP 16, 38042 Grenoble Cedex 9, France, and Département de Chimie Moléculaire, Equipe de Chimie Inorganique Rédox, CNRS, UMR 5250, Université Joseph Fourier, BP 53, 38041 Grenoble Cedex 9, France

Received June 18, 2007

Using magnetization measurements and multifrequency high-field electron paramagnetic resonance, the largest zero-field splitting for any individual isolated Mn^{II} ion has been found in a polyoxometalate complex, suggesting that the inorganic ligand induces large Ising-type magnetic anisotropy.

Polyoxometalates (POMs) represent an unique class of metal–oxygen complexes characterized by remarkable structures and properties that allow their use in numerous fields such as catalysis, magnetochemistry, photochemistry, materials science, and medicine.¹ While these species have been known for nearly two centuries, there is only a small number of cases where the POM acts as a ligand in transition-metal ion complexes. The electronic properties of some of these have been investigated² but not those of monosubstituted POM compounds.

We report here the first magnetic and high-field electron paramagnetic resonance (HF-EPR) investigation of a diamagnetic POM coordinated to a single paramagnetic ion. The magnetic center embedded in the POM ligand is found to possess an unusually high magnetic anisotropy. This result

shows that these systems offer a promising field for the investigation of Ising-type magnetic anisotropy, which has been intensively characterized in only mononuclear transition metal/organic ligand complexes so far.³

The complex $Rb_8[As_2W_{20}MnO_{68}] \cdot 36H_2O$ (**1**) was synthesized⁴ by mixing stoichiometric amounts of sodium tungstate, the $Na_{14}[As_2W_{19}O_{67}] \cdot 36H_2O$ ⁵ ligand, and manganese sulfate in hot water at $pH = 2–2.5$. Complex **1** was characterized by elemental analysis, IR and UV–vis spectroscopies,⁴ and single-crystal X-ray diffraction.⁶ Its structure (Figure 1) is analogous to those found for the previously reported Co and Zn derivatives.⁷

The three metallic sites forming the central belt are occupied by a Mn^{II} and two W^{VI} centers. The Mn^{II} ion is in a distorted square-pyramidal environment. Its equatorial plane contains four oxo ligands originating from the terminal O atoms of four $O=WO_5$ groups, and the axial position is occupied by a water molecule. A crystallographic C_3 axis

(3) Boca, R. *Coord. Chem. Rev.* **2004**, *248*, 257.

(4) Synthesis of **1**: in a 10 mL beaker, 2.520 g (4.5×10^{-4} mol) of $Na_{14}[As_2W_{19}O_{67}] \cdot 32H_2O$, 0.147 g (4.5×10^{-4} mol) of $Na_2WO_4 \cdot 2H_2O$, and 0.076 g (4.5×10^{-4} mol) of $Mn(SO_4)$ are dissolved in 5 mL of water at $T = 70–80$ °C. The pH of the mixture is adjusted to 2.2 with 1 M HCl, and the red solution is stirred for 15 min. After cooling to room temperature, 3 g (2.2×10^{-2} mol) of RbCl is added, and a few minutes later, the resulting orange precipitate is filtered and washed with 1 M KCl and dried with ethanol and ether. Yield: 2.1 g (85%). A total of 0.7 g of the powder are then recrystallized in 5 mL of water with gentle heating. After 1 night, 0.210 g of orange parallelepipedic crystals of **1** suitable for X-ray diffraction are obtained. IR (ν_{max}/cm^{-1}): 963s, 913sh, 878w, 768sh, 735vs, 640s, 507sh, 486m, 463m, 436m. UV–vis (H_2O): $\lambda = 390$ nm ($\epsilon = 1660$ mol⁻¹ L cm⁻¹). Anal. Calcd (found) for **1**: W, 58.34 (58.10); Mn, 0.87 (0.85); As, 2.38 (2.61); Rb, 10.85 (10.11).

(5) Tourné, C.; Tourné, G. *C. R. Acad. Sci., Ser. C* **1975**, *281*, 933.

(6) Crystal data for **1**: $Rb_8As_2W_{20}MnO_{104}H_{72}$, $M = 6302$, trigonal, $R\bar{3}$, $a = 20.238(1)$ Å, $c = 32.8668(3)$ Å, $V = 11412.50(13)$ Å³, $Z = 6$, $\rho_{calcd} = 3.029$ g cm⁻³, $\mu = 36.332$ mm⁻¹. 25 207 reflections measured, 6740 unique ($R_{int} = 0.0565$), $R1 = 0.0735$ and $wR2 = 0.1768$ [$I > 2\sigma(I)$], and $R1 = 0.0986$ and $wR2 = 0.1898$ (all data).

(7) Weakley, T. J. R. *Inorg. Chim. Acta* **1984**, *87*, 13.

* To whom correspondence should be addressed. E-mail: mialane@chimie.uvsq.fr (P.M.), duboc@grenoble.cnrs.fr (C.D.).

[†] Université de Versailles Saint-Quentin.

[‡] Université Paris-Sud.

[§] High Magnetic Field Laboratory, CNRS.

^{||} Université Joseph Fourier.

(1) (a) *Chemical Reviews, Polyoxometalates*; Hill, C. L., Ed.; American Chemical Society: Washington, DC, 1998. (b) *Polyoxometalate Chemistry for Nano-Composite Design*; Yamase, T., Pope, M. T., Eds.; Kluwer: Dordrecht, The Netherlands, 2002. (c) *Polyoxometalate Molecular Science*; Borrás-Almenar, J. J., Coronado, E., Müller, A., Pope, M. T., Eds.; Kluwer: Dordrecht, The Netherlands, 2004.

(2) (a) Kortz, U.; Nellutla, S.; Stowe, A. C.; Dalal, N. S.; Rauswald, U.; Danquah, W.; Ravot, D. *Inorg. Chem.* **2004**, *43*, 2308. (b) Mialane, P.; Duboc, C.; Marrot, J.; Rivière, E.; Dolbecq, A.; Sécheresse, F. *Chem.–Eur. J.* **2006**, *12*, 1950.

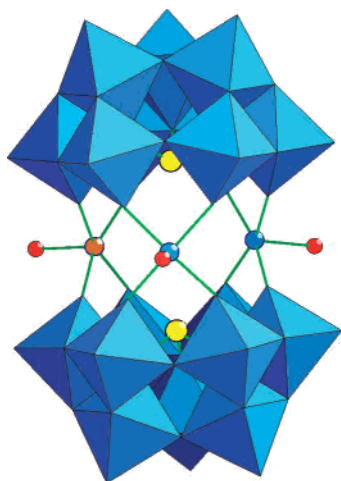


Figure 1. Polyhedral and ball-and-stick representation of the anion $[\text{As}_2\text{W}_{20}\text{MnO}_{68}]^{8-}$ in **1**. Color code: blue octahedra, WO_6 ; blue spheres, W; red spheres, O; yellow spheres, As; brown sphere, Mn.

induces a statistical disorder between the three metal ions forming the belt, thus preventing an accurate determination of the Mn–O distances. However, the coordination sphere of the Mn^{II} ion can be compared to that found in the complex $\text{K}_{11}\text{Na}[\text{As}_2\text{W}_{18}(\text{Mn}(\text{H}_2\text{O}))_3\text{O}_{66}]\cdot 27\text{H}_2\text{O}$, which we have previously reported.⁸ In this case, the belt is formed by three nondisordered Mn^{II} ions, with the Mn–O(W) and Mn–O(H_2) bond distances lying in the ranges 2.057(8)–2.082(7) and 2.157(14)–2.162(10) Å, respectively. In compound **1**, the Mn centers can be considered as magnetically isolated, with the shortest intermolecular $\text{Mn}^{\text{II}}\cdots\text{Mn}^{\text{II}}$ distance being 8.103(14) Å.

The electronic properties of complex **1** have been investigated by multifrequency EPR spectroscopy from 35 (*Q* band) to 285 GHz. Such high frequencies were required because of the unexpectedly large zero-field splitting (zfs) of this compound (see below).

A high-spin Mn^{II} ion ($3d^5$) is characterized by an electronic spin $S = 5/2$ and a nuclear spin $I = 5/2$. Its electronic properties can be described by the following Hamiltonian:

$$H = \beta B g S + I A S + D \left[S_z^2 - \frac{1}{3} S(S+1) \right] + E (S_x^2 - S_y^2) \quad (1)$$

The first two terms stand for the Zeeman and electron nuclear hyperfine interactions, respectively, while the two last terms define the zfs, with D and E denoting the axial and rhombic parts, respectively (the same sign for both D and E). The shape of the powder EPR spectra only depends on the zfs terms. The hyperfine structures cannot be observed, presumably because of intermolecular dipole–dipole interactions and D strain,⁹ which broaden the EPR lines. Furthermore, the g values are close to 2, owing to the quasi-spherical symmetry of the fundamental spectroscopic term of the Mn^{II} ion.¹⁰

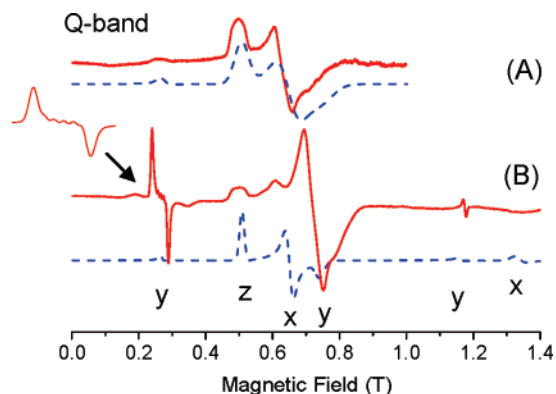


Figure 2. Experimental (solid red line) and simulated (dashed blue line) *Q*-band EPR spectra of complex **1** at 10 K. Part A was recorded immediately after placing the sample into the magnet at zero field. Part B was recorded following 3 min at 1.2 T. Simulations have been calculated as powder spectra using the parameters given in the text (line broadening: W, x, y, z = 500 G (A); 200 G (B)).

Figure 2 shows two *Q*-band EPR spectra recorded on a powder sample of complex **1**. Part A of Figure 2 was recorded immediately after the sample was placed into the magnet at zero field. The field was left at 1.2 T for 3 min, before recording part B of Figure 2. The following significant changes are observed: (i) the relative intensity of the 0.25 T lines is noticeably stronger in part B; (ii) the 0.25 and 1.15 T transitions present a derivative shape characteristic of an aligned single-crystal EPR spectrum in part B, whereas they exhibit an absorption mode corresponding to a powder spectrum in part A; (iii) the 0.25 T transition in part B is split into six equally spaced lines (82 G) originating from the hyperfine interaction with the nuclear spin of the Mn^{II} ion. These effects clearly show that the powder grains spontaneously orient in the magnetic field. This phenomenon is reversible: after shaking of the EPR tube, the single-crystal-like spectrum in part B converts back to the powder-like spectrum.

The presence of transitions between 0 and 1.4 T and the evidence for a torque effect between the magnetic field and the anisotropic magnetization in each grain indicate that D is large in **1**. We thus performed experiments at higher frequencies in order to analyze the *Q*-band EPR data.

A multifrequency EPR investigation (95, 115, 190, 230, and 285 GHz) established that the powder is preferentially aligned along the y magnetic axis of the molecule. We accurately determined the spin Hamiltonian parameters by using a full-matrix diagonalization procedure of eq 1 that simulates the EPR data recorded at all frequencies and temperatures:¹¹

$$D = +1.46(1) \text{ cm}^{-1}; E = +0.33(1) \text{ cm}^{-1}; E/D = 0.23; g_x = 2.01(1); g_y = 2.00(1), \text{ and } g_z = 2.02(1)$$

As an example, the 190 GHz EPR spectra recorded on a powder sample of **1** at 5 and 15 K are shown in parts A and B of Figure 3, respectively. At these high magnetic fields, the powder is oriented and the spectra display a single-

(8) Mialane, P.; Marrot, J.; Rivière, E.; Nebout, J.; Hervé, G. *Inorg. Chem.* **2001**, *40*, 44.

(9) Golombek, A. P.; Hendrich, M. P. *J. Magn. Reson.* **2003**, *165*, 33.

(10) *Electron paramagnetic resonance of transition ions*; Abragam, A., Bleaney, B., Eds.; Clarendon Press: Oxford, U.K., 1970.

(11) The simulation software SIM has been written by: Weihe, H. <http://sophus.kiku.dk/software/epr/epr.html>. See ref 12f.

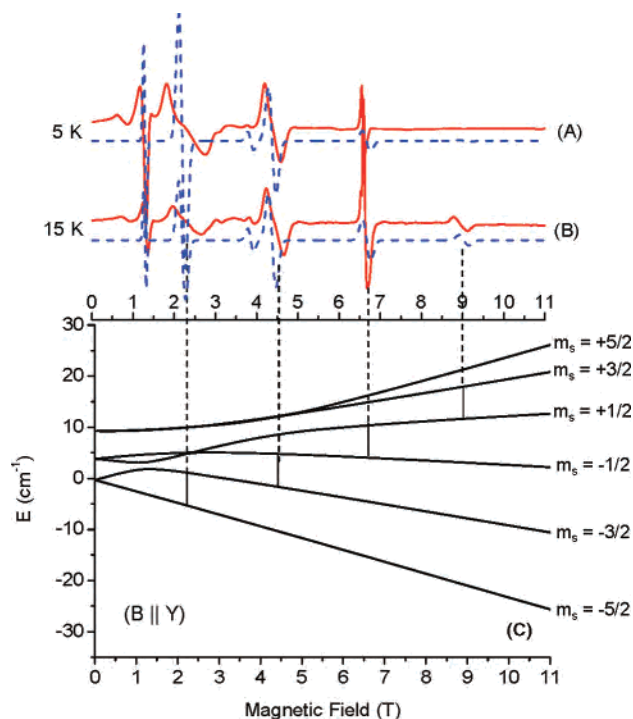


Figure 3. Experimental (solid red line) and simulated (dashed blue line) 190 GHz EPR spectra of complex **1** at 5 (A) and 15 (B) K. Simulations have been calculated using the parameters given in the text as a single-crystal-like spectrum along the y magnetic axis. (C) Plots of energy versus field for the six levels arising from an $S = 5/2$ spin state using the parameters given in the text. The field is parallel to the molecular y axis. Arrows indicate the observed resonances.

crystal-like shape. The transitions can be assigned (Figure 3C) from the energy level diagram arising from the $S = 5/2$ spin state of **1**. As expected from the Boltzmann population, the 8.9 T feature associated with the $|5/2, +1/2\rangle \rightarrow |5/2, +3/2\rangle$ transition only appears at 15 K, while at 5 K, only the three first Zeeman levels are populated.

The magnetization has been measured at $T = 2, 4,$ and 6 K as a function of the field on a polycrystalline powder sample of **1** pressed into a pellet in order to avoid preferential orientation of the crystallites. As can be seen in Figure 4, the following single set of fit parameters in the spin Hamiltonian (eq 1) reproduces the three magnetization curves very well:

$$|D| = 1.42 (1) \text{ cm}^{-1}; E/D = 0.20(1); g_{\text{iso}} = 1.99$$

The excellent agreement between the magnetic and EPR results confirms the unusually large value of $D = +1.46 \text{ cm}^{-1}$ for **1**. To our knowledge, this is the highest magnitude of D ever found for any individual isolated Mn^{II} ion. Such a high single-ion anisotropy was totally unexpected for a pentacoordinate Mn^{II} POM complex for two reasons.

First, the highest D values were previously known to occur in iodo complexes¹² ($|D| = 1.21 \text{ cm}^{-1}$ for $\text{trans-}[\text{Zn}(\text{Mn})(\text{N}_2\text{H}_4)_2(\text{I})_2]$ ^{12a}). Recent density functional theory calculations

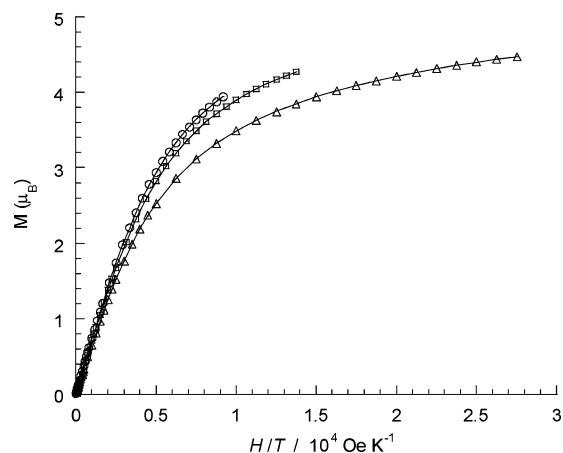


Figure 4. $M = f(H/T)$ plots at $T = 2$ (Δ), 4 (\square), and 6 (\circ) K for complex **1**. The solid lines were generated from the best-fit parameters given in the text.

have explained this observation by the stronger spin–orbit coupling of iodide as compared to other halides.^{12b}

Second, for complexes with only strong field ligands (O or N), the magnitude of D has been related to the coordination number of the ion. Because **1** and Mn^{II} /organic ligand complexes have similar Mn–O bond distances, a comparable D value would be expected, i.e., $0.2\text{--}0.4 \text{ cm}^{-1}$ (the observed range for pentacoordinate complexes).¹³

Therefore, we are led to the conclusion that the POM ligand embedding the paramagnetic center must play a crucial role in this large Ising-type magnetic anisotropy.

Experimental work on hexacoordinate Mn^{II} /polyoxotungstate systems and on a series of Mn^{II} halide polyoxomolybdate complexes¹⁴ is currently in progress in order to disentangle the various contributions to D .

Acknowledgment. The authors are grateful for financial support from Grant ANR-06-JCJC-0146-01 and to M.-H. Julien for critical reading of the manuscript.

Supporting Information Available: X-ray crystallographic data of **1** in CIF format and a figure showing the three-dimensional lattice of **1**. This material is available free of charge via the Internet at <http://pubs.acs.org>.

IC701193F

- (12) (a) Birdy, R. B.; Goodgame, M. *Inorg. Chim. Acta* **1981**, *50*, 183. (b) Duboc, C.; Phoeung, T.; Zein, S.; Pecaut, J.; Collomb, M.-N.; Neese, F. *Inorg. Chem.* **2007**, *46*, 4905. (c) Wood, R. M.; Stucker, D. M.; Jones, L. M.; Lynch, W. B.; Misra, S. K.; Freed, J. H. *Inorg. Chem.* **1999**, *38*, 5384. (d) Lynch, W. B.; Boorse, R. S.; Freed, J. H. *J. Am. Chem. Soc.* **1993**, *115*, 10909. (e) Mantel, C.; Baffert, C.; Romero, I.; Deronzier, A.; Pécaut, J.; Collomb, M.-N.; Duboc, C. *Inorg. Chem.* **2004**, *43*, 6455. (f) Jacobsen, C. J. H.; Pedersen, E.; Villadsen, J.; Weihe, H. *Inorg. Chem.* **1993**, *32*, 1216.
- (13) (a) Tabares, L. C.; Cortez, N.; Agalidis, I.; Un, S. *J. Am. Chem. Soc.* **2005**, *127*, 6039. (b) Mantel, C.; Philouze, C.; Collomb, M.-N.; Duboc, C. *Eur. J. Inorg. Chem.* **2004**, 3880. (c) Smoukov, S. K.; Telser, J.; Bernat, B. A.; Rife, C. L.; Armstrong, R. N.; Hoffman, B. M. *J. Am. Chem. Soc.* **2002**, *124*, 2318 and references cited therein.
- (14) Villanneau, R.; Proust, A.; Robert, F.; Gouzerh, P. *Chem.—Eur. J.* **2003**, *9*, 1982.